Published in final edited form as:
J Proteome Res. 2012 March 2; 11(3): 1913–1923. doi:10.1021/pr2011044.

Analysis of Tubulin Alpha-1A/1B C-Terminal Tail Post-translational Poly-glutamylation Reveals Novel Modification Sites

Ziad J. Sahab[*], **Alexander Kirilyuk**, **Lihua Zhang**, **Zahraa I. Khamis**, **Petr Pompach**, **YouMe Sung**, and **Stephen W. Byers**
Department of Oncology, Lombardi Comprehensive Cancer Center, Georgetown University, Washington, DC 20007, USA

Abstract

Tubulin-$\alpha_{1A/1B}$ C-terminal tail (CTT) has 7 glutamic acid residues among the last 11 amino acids of its sequence that are potential sites for glutamylation. Cleavage of C-terminal tyrosine resulting in the detyrosinated form of tubulin-$\alpha_{1A/1B}$ is another major modification. These modifications among others bring about highly heterogeneous tubulin samples in brain cells and microtubules, play a major role in directing intracellular trafficking, microtubule dynamics, and mitotic events, and can vary depending on the cell and disease state, such as cancer and neurodegenerative disorders. Identified previously using primary mass spectrometry (MS) ions and partial Edman sequencing, tubulin-$\alpha_{1A/1B}$ glutamylation was found exclusively on the E^{445} residue. We here describe the analysis of tubulin-$\alpha_{1A/1B}$ glutamylation and detyrosination after 2DE separation, trypsin and proteinase K in-gel digestion, and nanoUPLC-ESI-QqTOF-MS/MS of mouse brain and bovine microtubules. Tyrosinated, detyrosinated, and Δ2- tubulin-$\alpha_{1A/1B}$ CTTs were identified based on a comparison of fragmentation patterns and retention times between endogenous and synthetic peptides. Stringent acceptance criteria were adapted for the identification of novel glutamylation sites. In addition to the previously identified site at E^{445}, glutamylation on mouse and bovine tubulin-$\alpha_{1A/1B}$ CTTs was identified on E^{441} and E^{443} with MASCOT Expect values below 0.01. O-methylation of glutamates was also observed.

Keywords

AGBL2; Detyrosination; Glutamylation; Tandem hybrid mass spectrometry; Tubulin methylation; Microtubule Targetting Drugs (MTTDs); Nano-LC; Proteinase K; Tubulin-alpha; Tubulin C-terminal Tail

[*]Corresponding Author: Ziad J. Sahab, Georgetown University-Lombardi Comprehensive Cancer Center, 3970 Reservoir Rd NW Suite E415; Phone: 202-687-1891; Fax: 202-687-7505; zjs3@georgetown.edu.

Supporting Information Peak lists and raw mass spectral data associated with this manuscript may be downloaded in the original instrument vendor file format free of charge from ProteomeCommons.org Tranche, https://proteomecommons.org/Tranche/ using the following hash: fVyZLwkXWtMvOf6ntwzhcjKQ3e/I3TwEzV0lO/VYLU8aDLhHa28UIg3SiDf6s6P4KHOO7a QeG4bJNYVt7U4dYFkCJToAAAAAAAAATXg==
Supplementary Figures S1 to Figure S20, original MASCOT CID MS/MS annotated spectra including b, y, and internal fragments for synthetic and endogenous tubulin-$\alpha_{1A/1B}$ CTTs that were identified. Supplementary Table S1, list of common contaminants that were excluded from the Paragon search. Supplementary Table S2, the 12 mouse tubulin isoforms which were included in the custom MASCOT database. Supplementary Table S3, the 12 bovine tubulin isoforms which were included in the custom database. Supplementary Table S4, List of trypsin generated tubulin-$\alpha_{1A/1B}$ sequences that were identified following trypsin digestion by Paragon. Supplementary Table S5, List of trypsin generated tubulin-$\alpha_{1A/1B}$ sequences that were identified following trypsin digestion by MASCOT. Supplementary Table S6, List of excluded masses that were identified as possible matches to a random tubulin-$\alpha_{1A/1B}$ sequence. This material is available free of charge via the internet at http://pubs.acs.org

INTRODUCTION

Cytoskeletal proteins play a major role in the mitotic progression, spindle assembly, proper positioning of the nucleus, cell motility, actin filament growth, organelle biogenesis, mitochondrial tubulation, and suppression of telomere aberrations[1-12]. α and β-tubulins are the building blocks of the cytoskeletal microtubules. Tubulin-$\alpha_{1A/1B}$ incorporated in the microtubules has a CTT (…EGEGEEEGEEY^{451}) with seven glutamic acid residues that are potential sites for glutamylation, glycylation, and detyrosination[13]. Tubulin-$\alpha_{1A/1B}$ C-terminal tail (CTT) is the interaction site for many microtubule-binding proteins and newly-identified cytoskeletal interactors and regulators revealed a more pronounced role for the cytoskeleton in regulating cell functions[14-24]. The need to screen tubulin for its CTT modifications is very important because it is thought that tubulin modifications affect interactions with cytoskeletal-associated proteins and that different modifications generate a "tubulin code" similar to the biochemical model of the "histone code" on chromatin, regulating microtubule effectors and as a consequence dictating microtubule function, including the mitotic *modus operandi* in the cell important in diseases like cancer and neurodegenerative disorders[25, 26]. Furthermore, tubulin CTT is positioned at the outer lattice of microtubules/centrioles[25] suggesting that modification of this CTT plays a major role in the regulation of the dynamics of mitotic centrioles in addition to making them available for drug targeting (Figure 1).

Tubulin-$\alpha_{1A/1B}$ detyrosination refers to the reversible removal of the CTT residue by the recently identified putative tubulin carboxypeptidase AGBL2[27]. Tyrosine reincorporation is carried out by the tubulin tyrosine ligase (TTL) enzyme[28]. A third tubulin-$\alpha_{1A/1B}$ isotype lacking tyrosine and glutamate C-terminal residues, referred to as Δ2-tubulin, was found to be present in cancer cells and absent in all normal tissues except the brain[29]. Polyglutamylation occurs by covalent bonding to the γ-carboxylate group of glutamates present at the tubulin-$\alpha_{1A/1B}$ CTTs by tubulin tyrosine ligase like (TTLL) poly(glutamylases)[30].

Although several specific antibodies have been generated to a number of modified tubulin peptides, as is the case with antibodies to specific histone modifications, for the most part these antibodies will not detect peptides that have modifications in addition to the sequence which the antibody was raised against. As multiply-modified tubulin-$\alpha_{1A/1B}$ CTT peptides are the rule rather than the exception[31], LC/MS-MS offer the best chance of simultaneously detecting multiple peptide modifications. However this sort of analysis is hindered by the dynamic and heterogeneous nature of the CTT of tubulin-$\alpha_{1A/1B}$ as well as the large molecular mass of that CTT produced after digestion using different enzymes[32, 33]. Identified in 1990 using primary mass spectrometry (MS) ions following digestion with thermolysin, and methylation of glutamate's side chain carboxylic acid, tubulin-$\alpha_{1A/1B}$ glutamylation was found exclusively on E^{445} via partial Edman sequencing of the CTT sequence starting with V^{440} to E^{448} [34, 35]. Tubulin-$\alpha_{1A/1B}$ CTT glutamylations have subsequently been identified based on their primary ion masses that cannot afford to localize the glutamylation site[31-33, 35-37]. Recently, MS/MS spectra were generated for glutamylated tubulin-α1 CTT of pathogen *toxoplasma gondii* (…GEEEGYGEDY^{453}) that differs from tubulin-$\alpha_{1A/1B}$ CTT of mouse (*mus musculus*) and cows (*bos taurus*) also conserved in humans (*homo sapiens*)(…EGEGEEEGEEY^{451})[38]. That accounted for the only MS/MS spectra of endogenous glutamylated tubulin-α_1 that was found in the literature.

We here describe the use of sequential trypsin and proteinase K digestion coupled with nanoUPLC-ESI-QqTOF-MS/MS to re-explore tubulin-$\alpha_{1A/1B}$ CTT detyrosination and glutamylation in mouse brain. Tubulin-$\alpha_{1A/1B}$ CTT peptides with molecular masses in the range of 964-1256 Da were generated following trypsin and proteinase K digestion. CID

MS/MS spectra for endogenous mammalian glutamylated tubulin-$\alpha_{1A/1B}$ CTTs were generated and compared to those of synthetic peptides and identification of previously undetected tubulin-$\alpha_{1A/1B}$ glutamylation sites was granted. Our findings were validated using a purified bovine brain microtubule sample. Our data is complemental to the earliest findings in the area of tubulin glutamylation by Edde *et al*[34].

EXPERIMENTAL PROCEDURES

The mouse used in this study, C57BL/6J was obtained from Jackson Laboratory and kept under standard laboratory conditions. The Animal Care Committee (ACC) approved all experimental procedures that relates to this project. The mouse was killed under anesthesia at the age of 8 months and underwent encephalectomy. Bovine brain microtubules (99% pure) were purchased from Cytoskeletton, Inc. (Denver, CO). C-terminal tails (CTT) of the following tubulin-$\alpha_{1A/1B}$ isotypes were custom-synthesized at Genscript (Piscataway, NJ) with > 95% purity: tyrosinated (EGEGEEEGEEY), Detyrosinated (EGEGEEEGEE), and Δ2 (EGEGEEEGE).

Mouse Brain Protein Extraction and Quantitation

Mouse brain was washed 3 times with ice-cold PBS followed by mashing in 1 mL of ice-cold tissue lysis buffer composed of 10 mM Tris, 130 mM NaCl, 1% octylglucopyranoside (OG), 1% CHAPS, 10 mM sodium phosphate, and 10 mM sodium fluoride (pH 7.5). This was succeded by vortexing and centrifugation as described previously[39]. This resulted in the formation of 3 layers: the top layer was composed primarily of non-soluble lipids, the middle layer contained the soluble proteins, and the bottom layer was composed of cell debris. The middle layer was recovered and used for subsequent analyses. Proteins were quantified using the BCA assay as described previously[40].

Western Blotting

Western Blotting was performed using a mouse monoclonal anti-tubulin-α (Clone B-5-1-2; Sigma, St Louis, MO) as described previously[41].

Two-Dimensional Gel Electrophoresis (2-DE) and Staining

2-DE gel was utilized to separate 50 μg of total brain lysates or purified microtubules using a pH 4 to 7 or 3 to 10 IPG strips for the first dimension and a 4-12% PAGE gel in the second dimension as described previously[42]. Coomassie blue staining was performed by fixing the gel first in 50% methanol (v/v) and 12% acetic acid (v/v) for 2 hours, followed by incubation in Coomassie Blue solution. Background destaining was accomplished by incubating the gel in the fixing solution.

Gel Excision, trypsin Digestion, and ESI-TOF/TOF Analysis

Gel excision and trypsin digestion were performed as described previously[43]. Following overnight incubation with trypsin, samples were sonicated for 30 minutes, tryptic digests were desalted as described previously[44] and analyzed by nanoUPLC-ESI-QqTOF-MS/MS as described below.

Identification of 2DE Spots

GPS Explorer v3.6 (Applied Biosystems, Foster city, CA) default parameters and thresholds were used to create the peak list from the raw data of trypsin digests. ProteinPilot 3.0 (Applied Biosystems, Foster city, CA) was used to submit the data to Paragon v3.0 algorithm with the following settings: Database: *mus musculus* for the mouse brain sample (NCBInr + SwissProt with ~165,000 protein entries) and *bos taurus* for the bovine sample

(SwissProt with ~39,000 protein entries). Common contaminants like trypsin and keratins listed in Table S1 were excluded from the search; Sample Type: Identification; Cys Alkylation: Iodoacetamide; Digestion: Trypsin; Species: *mus musculus*; Settings for missed cleavages, mass tolerance for precursor and fragment ions are removed in Paragon v3.0 that uses instrument-dependent defaults for these settings. Paragon v3.0 protein identifications and MS/MS spectra were accepted when the algorithm -generated unused protein and individual ion scores were above 1.3 corresponding to a confidence interval above 95% indicating that the probability of a random match is lower than 5%. False positive rates were not generated as this analysis was performed on individual 2DE spots and because the protein of interest is highly abundant in the sample. MS and MS/MS data were also submitted to MASCOT to identifiy 2DE spots using the same search parameters as above in addition to limiting the mass tolerance to 0.2 Da for both precursor and fragment ions. Only one missed cleavage was allowed.

NanoUPLC-ESI-QqTOF-MS/MS Analysis of Proteinase K Digests and Synthetic Peptides

Remaining trypsin digests of the 2DE spots that were identified as tubulin-$\alpha_{1A/1B}$ were transferred to a centrifuge tube and subjected to an additional digestion step by adding 1μL of a 1μg/μL proteinase K solution. The mixture was incubated overnight at 37°C. Synthetic peptides and Proteinase K digests were separated utilizing a nanoACQUITY nano-UltraPerformance-LC System (Waters, Milford, MA) with reversed phase column BEH C18 column 1.7 μm, 75 μm × 150 mm (Waters). Peptides were eluted over 30 min linear gradient of 0-60% of solvent B (98% acetonitrile, 0.1% formic acid) at a flow rate of 400 nL/min. Solvent A was composed of 2% acetonitrile and 0.1% formic acid. The nanoUPLC system was coupled to a QStar Elite® mass spectrometer equipped with NanoSpray II ionsource (AB Sciex, Framingham, MA). Eluted peptides were ionized in the positive mode using a fused silica PicoTip emitter with an outer diameter measuring 75 μm and an inner diameter of 15 μm for the emitter orifice (New Objective, Woburn, MA). A spray voltage of 2300 V, a curtain gas of 13 psi, a nebulizer gas of 13 psi, an interface heater temperature of 180°C were set for this analysis.

Identification of tubulin-$\alpha_{1A/1B}$ CTTs

MS and MS/MS data generated for the proteinase K digests were searched against the whole mouse and bovine databases using the settings described above while specifying proteinase K as the digesting enzyme. A custom-built database composed of 12 mouse (Table S2) or12 bovine (Table S3) tubulin-α and β isoforms using MASCOT v2.2 search engine (http://www.matrixscience.com) (Matrix Sciences, London, UK) in ProteinPilot 3.0 software (AB Sciex) using default parameters for peak picking with a mass tolerance of 0.2 Da for precursor and for fragment ions. Mass spectra were individually inspected to confirm the monoisotopic peak assignments. Fixed modifications: None; Variable modifications: Carbamidomethyl (C); Oxidation (M); Methylation of Carboxylic acids (ED and C-terminal), and the addition of 1 to 3 glutamate residues on glutamates. MASCOT configuration was modified to identify E modification by E, and multiple neutral losses of 18 Da (water) from primary and secondary ions that were observed on the CID MS/MS spectra of synthetic peptides. Pyroglutamylation was not discernible from dehydration (-18 Da) Enzyme specificity: Proteinase K; missed cleavages: 0; Taxonomy: Unclassified.

Acceptance criteria for tubulin-$\alpha_{1A/1B}$ CTT MS/MS Hits

The following criteria were adopted for MASCOT-annotated MS/MS spectra: (1) All m/z that were identified as belonging to random tubulin-$\alpha_{1A/1B}$ non-CTT peptides were excluded; (2) NanoUPLC retention times within 1 min. (400 nL) of that of synthetic peptides; (3) Fragmentation pattern comparable to that of synthetic peptides; (4) for regular identification, MASCOT Expect value < 0.05 indicating that the probability of a random

match is < 5%; (5) for the identification of novel glutamylation sites, MASCOT Expect value < 0.01 indicating that the probability of a random match is < 1%; (6) >90% CTT sequence coverage; (7) Error < 0.2 Da for precursor and fragment ions; (8) In cases where the second isotope was picked, the error allowed was 1 Da ± 0.2; (9) MASCOT ion score of at least 14 corresponding to a confidence interval of at least 95%.

Differentiating Endogenous Modifications from Artifactual Ones

Synthetic tyrosinated tubulin-$\alpha_{1A/1B}$ CTT was subjected to the experimental conditions that endogenous tubulin went through to identify the modifications that are caused by sample preparation. The CTT was mixed with DTT and incubated for 1 hour at 56°C, iodoacetamide was then added and the mixture was incubated in the dark for 30 min at room temperature. Coomassie Blue and its destaining solution containing methanol and acetic acid were then added to the mixture and incubated for 3 hours. The mixture was then diluted 10,000 fold prior to nanoLC injection to reduce the amount of methanol and acetic acid that are injected therefore avoiding any damage to the C18 nano column. MS and MS/MS spectra were then generated as described above.

RESULTS AND DISCUSSION

Study Design

Whole mouse brain protein extracts and were separated on 2DE. A pure bovine microtubule sample was similarly analyzed to rule out any data interference from molecules other than tubulins[45-52]. Spots were excised, trypsin digested and subjected to ESI-TOF/TOF. Spots that were reliably identified as tubulin-$\alpha_{1A/1B}$ with Paragon confidence interval of 99% (Table S4) and MASCOT scores up to 495 (Table S5) on the basis of unmodified peptides underwent a second digestion with proteinase K. The double digestion of tubulin-$\alpha_{1A/1B}$ preserved the CTT peptides of tubulin-$\alpha_{1A/1B}$ while at least theoretically reducing the remaining tubulin-$\alpha_{1A/1B}$ sequences to peptides with molecular masses lower than 1000 Da allowing for a relatively cleaner MS spectrum in the CTT mass range when analyzed by nanoUPLC-ESI-QqTOF-MS/MS. MS and MS/MS data generated for the trypsin/proteinase K double digested tubulins were searched against the whole mouse/bovine databases and their identities were confirmed as tubulin-$\alpha_{1A/1B}$. A MASCOT v2.2 custom-database containing 12 tubulin isoforms (Table S2) was then created to restrict the search space for glutamylation. The following variable modifications were created in MASCOT v2.2 software configurations: +1E(E); +2E(E); and +3E(E) to account for the (poly)glutamylation modifications of glutamic acids. Detection of multiple neutral losses of 18Da from primary and secondary ions corresponding to the dehydration of the glutamates' carboxylic acid groups as seen on the CID MS/MS spectra of synthetic peptides was also adapted on MASCOT. The study was repeated using a 99% pure bovine brain microtubule sample (Cytoskeletton Inc., Denver, CO) to validate the findings.

Protein Separation and Tubulin-$\alpha_{1A/1B}$ Identification

Mouse brain protein extracts was separated on 2DE followed by Coomassie blue staining (Figure 2A). Western blotting against tubulin-α was also performed to localize the proteins of interest. Several tubulin-α isoforms were recognized by the antibody (Figure 2B). A bovine microtubule protein sample was also separated on 2DE (Figure 2C). Matching spots that were recognized by western blot were excised from the 2D gel, destained, trypsin-digested, and analyzed by ESI-Q-TOF/TOF. Several spots were identified as tubulin-$\alpha_{1A/1B}$ following analysis of tryptic digests with a high confidence interval based on non-CTT peptide identification (Figure 2D) (Table S4, S5). The high CI is not surprising since tubulins are highly abundant in microtubules and in brain cells [31, 33, 35]. Spots that were identified as tubulin-$\alpha_{1A/1B}$ by MS and MS/MS following trypsin digestion underwent a

second digestion with proteinase K. The double digestion allowed for the generation of tubulin-$\alpha_{1A/1B}$ CTT peptides with theoretical molecular masses in the range of 964 - 1256 Da. Theoretical masses were computed using PeptideMass tool of expasy (http://web.expasy.org/peptide_mass/). While this tool only accepts one enzyme at a time, the enzyme entry that was utilized to generate the theoretical masses was proteinase K since it cleaves the C-terminal of V^{440} which is closer to the C-terminal of the protein than the last peptide bond cleaved by trypsin at K^{430}. Theoretically, tubulin CTT will have the highest molecular mass among all peptides generated by trypsin and proteinase K digestion of tubulin-$\alpha_{1A/1B}$ and since these CTTs have only one amino group (N-terminal), their theoretical m/z should be 1256.4 Da for tyrosinated, 1093.4 Da for detyrosinated and 964.4 Da for Δ2 tubulin-$\alpha_{1A/1B}$ as they should be singly charged. An additional data purification step was performed to account for missed cleavages or non-specific proteolysis that may yield non-CTT ions with masses close to those of the CTTs. CID MS/MS spectra were scanned against the sequences of tubulin-$\alpha_{1A/1B}$ without specifying any enzymes. All peptides that were identified as belonging to random non-CTT tubulin-$\alpha_{1A/1B}$ fragments within an error of 0.2 Da for primary and fragment ions were excluded even if the sequence is not a usual product of trypsin or proteinase K digestion. Excluded masses are listed in Table S6 with their corresponding random tubulin-$\alpha_{1A/1B}$ fragments.

Fragmentation Patterns of Synthetic Peptides and Dehydration of Glutamates

EGEGEEEGEEY is the tyrosinated CTT generated by the double digestion of trypsin and proteinase K according to the PeptideMass tool of Expasy. Synthetic peptides corresponding to the CTT of tyrosinated (EGEGEEEGEEY), detyrosinated (EGEGEEEGEE), and Δ2 (EGEGEEEGE) tubulin-$\alpha_{1A/1B}$ were custom-synthesized (Genscript, Piscataway, NJ). Having only one amino group (N-terminal), these peptides were supposed to be singly-charged following electrospray ionization (ESI). When the synthetic tyrosinated CTT was analyzed by NanoUPLC-ESI-QqTOF-MS/MS, the main MS ion was surprisingly doubly charged with an $[M+2H]^{2+}$ (m/z 628.6973) (Figure 3A). The singly charged ion was also present (MH^+/m/z 1256.3318) at a lower intensity. Dehydrated primary ions were also observed on the spectrum: Neutral loss of 1 water molecule was observed in both singly charged $[M+H-H_2O]^+$ (m/z 1238.3943) and double charged $[M+2H-H_2O]^{2+}$ (m/z 619.7092) ions. Neutral losses of up to 7 water molecules were also detected for both ions: $[M+2H-7H_2O]^{2+}$ (m/z 565.1917); $[M+H-7H_2O]^+$ (m/z 1130.3228). MS/MS spectra of $[M+2H-H_2O]^{2+}$ (m/z 619.7092) showed 3x18Da neutral losses for b6 (m/z 631.2013) and 2x18Da losses for b5 fragments (m/z 502.1431) (Figure 3B). A pattern of 7 peaks from m/z 466.1294 to m/z 574.1637 with a ΔM of 18Da was also observed. Neutral losses of multiple 18Da are indicative of the dehydration of γ-carboxylic acid groups of glutamates. The same phenomenon was also observed for detyrosinated and Δ2-tubulin-$\alpha_{1A/1B}$. Since this artifactual modification is significantly affecting the mass distribution of both primary and secondary ions, MASCOT was adapted to recognize it. MASCOT was also set to identify internal fragments that were abundantly produced during the fragmentation of the synthetic peptides (Figures S1-S3). The effect of glutamate on the fragmentation mode of peptides has been extensively studied. Early studies showed that glutamates undergo dehydration and deamidation during the fragmentation process resulting in the formation of pyroglutamic acid[53]. Other studies showed that fragmentation of glutamate-containing peptides results in cyclic cationated anhydrides or imide ions[54]. Neutral losses of water happen during the fragmentation of the precursor ions. While MS/MS spectra were published for (poly)glycylated α-tubulins[55], the only account in the literature of an endogenous glutamylated α-tubulin MS/MS spectrum belongs to *Toxoplasma gondii* (pathogen) which tubulin CTT structure differs from that of mammalians[38]. More recently T^3-sequencing was successful at differentiating tubulin-$\alpha_{1A/1B}$ from other α-tubulin isoforms but did not address tubulin glutamylation[56].

Identification of Endogenous Tyrosinated, Detyrosinated and Δ2-Tubulin-$\alpha_{1A/1B}$ CTTs

All identified CTTs are listed in Table 1 (mouse) and Table 2 (bovine). All original MASCOT-generated spectra and identifications are shown in the supplementary materials (Figures S1-S20). MS/MS fragmentation ions of proteinase K digested gel spots that were identified as tubulin-$\alpha_{1A/1B}$ were searched against the sequences of 12 different tubulin isoforms with the variable modification of E (up to 3E) addition to E, methylation of E, and neutral losses of multiple 18Da. Counting on the well-established MASCOT scoring system to accept or reject MS/MS hits was the mainstay of our identifications. Our acceptance criteria were stringent and required a MASCOT Expect value < 0.05 for regular identification indicating that the probability of a random match is < 5% and a MASCOT Expect value < 0.01 for the identification of novel glutamylation sites indicating that the probability of a random match is < 1%; sequence coverage of more than 90%; difference between retention times of endogenous and synthetic peptides lower than 1 min.; Error < 0.2 Da for precursor and fragment ions. Our detailed acceptance criteria are described in the experimental procedures section. Mouse brain endogenous tyrosinated (Figure 4A), detyrosinated (Figure 4B), and Δ2- (Figure 4C) tubulin-$\alpha_{1A/1B}$ CTTs were identified based on standard b and y-type fragmentation products that were picked by MASCOT v2.2. Bovine tubulin CTTs were similarly identified (Fig. S14, S15, S16). Fragmentation patterns were similar to those of synthetic peptides after accounting for the methylation on endogenous tubulins and the differential dehydration that occurred between endogenous and synthetic peptides. Retention times of the nanoUPLC chromatography were also collected for each ion and compared with that of the synthetic peptide to confirm the identities of the CTTs. Endogenous tyrosinated CTT eluted at 13.74 min versus 14.01 min for the synthetic CTT (Figure 4A). Endogenous detyrosinated and Δ2- CTTs eluted at 11.80 (Figure 4B) and 11.38 min (Figure 4C) which are comparable to the retention times of the synthetic ions: 11.39 and 11.04 min. respectively.

Identification of Glutamylated Tubulin-$\alpha_{1A/1B}$ CTTs

Tubulin-$\alpha_{1A/1B}$ CTT glutamylation was identified on E^{445} by Edde *et al* following Edman sequencing. A gap in sequencing at E^{445} indicated the presence of a modified E^{445} residue[34]. This work was later confirmed after performing Edman sequencing on an isolated tubulin-$\alpha_{1A/1B}$ CTT[57]. Edman sequencing was considered the primary method for sequence identifications, but its sensitivity is far inferior to current instrumentation. Edman sequencing will disclose the sequence of the most abundant peptide in a sample that contains 2-3 peptides and while DEAE isolation of CTTs with different glutamylation states was utilized to purify individual CTTs prior to sequencing in the above-mentioned work, peptides with the same number of glutamic acid additions would have eluted together regardless of the position of the glutamylation site. The previously reported glutamylation site at E^{445} [34, 35] was identified (Figures S9, S12, S19) although this identification was ambiguously assigned on E^{445}, E^{446}, or E^{447} as modification of any of these 3 consecutive glutamates would have had the same fragmentation profile. Glutamylation of E^{441} was observed on tyrosinated (Figures S11, S20), detyrosinated (Figures 5A, S7, S17) with a MASCOT Expect value < 0.01 for all MS/MS hits. Glutamylation of E^{443} was also observed on detyrosinated tubulin (Figure 5B, S8, S18) and tyrosinated tubulin (Figure S13) with MASCOT Expect values lower than 0.01. Bi-glutamylation was observed on E^{441} (Figure S10) with a $p = 0.0032$. All of the identified glutamylated detyrosinated CTTs eluted at a retention time between $t_R = 11.59$ min. and $t_R = 12.43$ min. (Figure 6) close to the retention time of the synthetic detyrosinated CTT (11.39 min.) further supporting their identification as tubulin-$\alpha_{1A/1B}$ CTT isotypes since those were shown to elute at close retention times when separated using reverse-phase chromatography[57]. It is important to note that tyrosinated and detyrosinated tubulin CTT ionize differently and that a comparison of their respective MS signal will not yield an accurate ratio of their distribution in the sample[31].

The quantitation of the different tubulin modifications requires the use of a triple quadrupole MS and of an internal standard composed of a synthetic CTT with a heavy. Additional searches using different parameters identified other modifications but with lower scores and higher Expect values, namely modification of E^{449}/E^{450}, tri-, tetra-, and penta-glutamylations and were therefore considered a random match.

Differentiating Endogenous from Artifactual Modifications

Endogenous O-methylation of glutamic acids present at the CTT of tubulin-α was recently reported[38]. Methylation of Glutamates has also been reported to occur secondary to Coomassie Blue staining, mainly caused by the exposure to the methanol and acetic acid mixture which are part of the staining and destaining solutions[58]. Synthetic tyrosinated tubulin-$\alpha_{1A/1B}$ CTT was subjected to the experimental conditions that endogenous tubulin went through to identify the modifications that are caused by sample preparation. In addition to incubating the CTT with methanol and acetic acid, it was also incubated with DTT and iodoacetamide to mimick the experimental conditions. NanoLC-MS spectrum of the mixture was then generated (Figure 7). Singly charged ($[MH]^+$, m/z 1256.4396) and double charged ($[M+2H]^{2+}$; m/z 628.7290) tyrosinated tubulin-$\alpha_{1A/1B}$ were detected. The only artifactual modifications that were identified are dehydration and/or pyroglutamylation ($[M+2H-H_2O]^{2+}$; m/z 619.7720). Formation of standard adducts with sodium ($[M+H+Na]^{2+}$; m/z 639.7110); potassium ($[M+H+K]^{2+}$; m/z 647.7069); iron ($[M-H+Fe^{III}]^{2+}$ m/z 655.1817) was also observed. Methylation of glutamic acids was not observed. This point to the possibility of O-methylation occurring endogenously in agreement with recent work by Xiao et al who demonstrated the endogenous methylation of tubulin CTT glutamates in *Toxoplasma gondii*[38].

CONCLUSIONS

Sequential trypsin and proteinase K digestion are advantageous over other enzymes in terms of preserving the CTT of tubulin-$\alpha_{1A/1B}$ while reducing the remaining tubulin-$\alpha_{1A/1B}$ sequences to small peptides. Tyrosinated, detyrosinated, and Δ2-tubulin-$\alpha_{1A/1B}$ CTTs were identified following the double digestion of the 2DE spots. Other tubulin isoforms (e.g. Δ4-tubulin) were shown to carry (poly)glutamylation chains on more than one site[31]. The latter precedent supports the possibility of multiple glutamylation sites on tubulin-$\alpha_{1A/1B}$ CTT. Our study unambiguously identifies E^{441} and E^{443} as glutamylation sites in mouse and bovine brain tubulin-$\alpha_{1A/1B}$. Glutamylation could not be accurately assigned on E^{445}, E^{446}, and E^{447} where modification of at least one of these three consecutive E residues was observed. O-methylation of glutamates at the CTT of tubulin-$\alpha_{1A/1B}$ was also detected in endogenous peptides but not in control synthetic ones that were subjected to the same experimental conditions strongly suggesting that methylation is occurring endogenously. This method is biologically useful to analyze the regulation of the different tubulin-$\alpha_{1A/1B}$ glutamylation/detyrosination isotypes in biological samples and will be an important analysis tool in the research areas of cancer and neurodegenerative disorders. Identification of differential CTT modifications in tubulins is mainly important in the research area of cancer therapeutics. In fact microtubule targeting drugs (MTTDs/Chemotherapy) target a sequence of β-tubulin present in all microtubules including neuronal microtubules[59, 60]. Neuropathy secondary to MTTD treatment is the ensuing consequence. Research is underway to identify novel therapies to replace current MTTDs[61, 62]. Tubulin-$\alpha_{1A/1B}$ CTT is the most heterogeneous part of the microtubule making the identification of disease specific CTT -which targeting minimizes side effects- a possibility.

Supplementary Material

Refer to Web version on PubMed Central for supplementary material.

Acknowledgments

This study was supported in part by NIH R01CA129813, NIH 1 P01 CA130821 (SWB) and by the Charles and Mary Latham Fund (ZJS). The authors wish to acknowledge the support of the following Lombardi Comprehensive Cancer Center Core Facilities (NIH P30 CA51008): Animal and Proteomics shared resources.

References

1. Chen HC, Vermulst M, Wang YE, Chomyn A, Prolla TA, McCaffery JM, Chan DC. Mitochondrial Fusion Is Required for mtDNA Stability in Skeletal Muscle and Tolerance of mtDNA Mutations. Cell. 2010; 141(2):280–289. [PubMed: 20403324]
2. Ban T, Heymann JAW, Song ZY, Hinshaw JE, Chan DC. OPA1 disease alleles causing dominant optic atrophy have defects in cardiolipin-stimulated GTP hydrolysis and membrane tubulation. Human Molecular Genetics. 2010; 19(11):2113–2122. [PubMed: 20185555]
3. Cheli VT, Daniels RW, Godoy R, Hoyle DJ, Kandachar V, Starcevic M, Martinez-Agosto JA, Poole S, DiAntonio A, Lloyd VK, Chang HC, Krantz DE, Dell'Angelica EC. Genetic modifiers of abnormal organelle biogenesis in a Drosophila model of BLOC-1 deficiency. Human Molecular Genetics. 2010; 19(5):861–878. [PubMed: 20015953]
4. Folker ES, Ostlund C, Luxton GWG, Worman HJ, Gundersen GG. Lamin A variants that cause striated muscle disease are defective in anchoring transmembrane actin-associated nuclear lines for nuclear movement. Proceedings of the National Academy of Sciences of the United States of America. 2011; 108(1):131–136. [PubMed: 21173262]
5. Levi SK, Bhattacharyya D, Strack RL, Austin JR, Glick BS. The Yeast GRASP Grh1 Colocalizes with COPII and Is Dispensable for Organizing the Secretory Pathway. Traffic. 2010; 11(9):1168–1179. [PubMed: 20573068]
6. Ems-McClung SC, Walczak CE. Kinesin-13s in mitosis: Key players in the spatial and temporal organization of spindle microtubules. Seminars in Cell and Developmental Biology. 2010; 21(3): 276–282. [PubMed: 20109574]
7. Franke JD, Montague RA, Kiehart DP. Nonmuscle myosin II is required for cell proliferation, cell sheet adhesion and wing hair morphology during wing morphogenesis. Developmental Biology. 2010; 345(2):117–132. [PubMed: 20599890]
8. Lue NF. Plasticity of telomere maintenance mechanisms in yeast. Trends in Biochemical Sciences. 2010; 35(1):8–17. [PubMed: 19846312]
9. Mackay DR, Makise M, Ullman KS. Defects in nuclear pore assembly lead to activation of an Aurora B-mediated abscission checkpoint. Journal of Cell Biology. 2010; 191(5):923–931. [PubMed: 21098116]
10. Pollock C, Daily K, Van TN, Wang C, Lewandowska MA, Bensaude O, Huang S. Characterization of MRP RNA-protein interactions within the perinucleolar compartment. Molecular Biology of the Cell. 2011; 22(6):858–867. [PubMed: 21233287]
11. Weinger JS, Qiu MH, Yang G, Kapoor TM. A Nonmotor Microtubule Binding Site in Kinesin-5 Is Required for Filament Crosslinking and Sliding. Current Biology. 2011; 21(2):154–160. [PubMed: 21236672]
12. Sahab ZJ, Man YG, Byers SW, Sang QXA. Putative Biomarkers and Targets of Estrogen Receptor Negative Human Breast Cancer. International Journal of Molecular Sciences. 2011; 12(7):4504–4521. [PubMed: 21845093]
13. Westermann S, Weber K. Post-translational modifications regulate microtubule function. Nature Reviews Molecular Cell Biology. 2003; 4(12):938–947.
14. Joglekar AP, Bloom KS, Salmon ED. Mechanisms of force generation by end-on kinetochore-microtubule attachments. Current Opinion in Cell Biology. 2010; 22(1):57–67. [PubMed: 20061128]
15. Jin Y, Eves PT, Tang F, Weisman LS. PTC1 Is Required for Vacuole Inheritance and Promotes the Association of the Myosin-V Vacuole-specific Receptor Complex. Molecular Biology of the Cell. 2009; 20(5):1312–1323. [PubMed: 19116310]

16. Bayly PV, Lewis BL, Kemp PS, Pless RB, Dutcher SK. Efficient Spatiotemporal Analysis of the Flagellar Waveform of Chlamydomonas reinhardtii. Cytoskeleton. 2010; 67(1):56–69. [PubMed: 20169530]

17. Charest PG, Shen ZX, Lakoduk A, Sasaki AT, Briggs SP, Firtel RA. A Ras Signaling Complex Controls the RasC-TORC2 Pathway and Directed Cell Migration. Developmental Cell. 2010; 18(5):737–749. [PubMed: 20493808]

18. Compton DA. Mechanisms of aneuploidy. Current Opinion in Cell Biology. 2011; 23(1):109–113. [PubMed: 20810265]

19. Kueh HY, Brieher WM, Mitchison TJ. Quantitative Analysis of Actin Turnover in Listeria Comet Tails: Evidence for Catastrophic Filament Turnover. Biophysical Journal. 2010; 99(7):2153–2162. [PubMed: 20923649]

20. Subramanian R, Wilson-Kubalek EM, Arthur CP, Bick MJ, Campbell EA, Darst SA, Milligan RA, Kapoor TM. Insights into Antiparallel Microtubule Crosslinking by PRC1, a Conserved Nonmotor Microtubule Binding Protein. Cell. 2010; 142(3):433–443. [PubMed: 20691902]

21. Harris ES, Gauvin TJ, Heimsath EG, Higgs HN. Assembly of Filopodia by the Formin FRL2 (FMNL3). Cytoskeleton. 2010; 67(12):755–772. [PubMed: 20862687]

22. Banerjee A, Panosian TD, Mukherjee K, Ravindra R, Gal S, Sackett DL, Bane S. Site-Specific Orthogonal Labeling of the Carboxy Terminus of alpha-Tubulin. Acs Chemical Biology. 2010; 5(8):777–785. [PubMed: 20545322]

23. Noris P, Perrotta S, Seri M, Pecci A, Gnan C, Loffredo G, Pujol-Moix N, Zecca M, Scognamiglio F, De Rocco D, Punzo F, Melazzini F, Scianguetta S, Casale M, Marconi C, Pippucci T, Amendola G, Notarangelo LD, Klersy C, Civaschi E, Balduini CL, Savoia A. Mutations in ANKRD26 are responsible for a frequent form of inherited thrombocytopenia: analysis of 78 patients from 21 families. Blood. 2011; 117(24):6673–6680. [PubMed: 21467542]

24. Tsai F-M, Wu C-C, Shyu R-Y, Wang C-H, Jiang S-Y. Tazarotene-Induced gene 1 Inhibits Prostaglandin E2-Stimulated HCT116 Colon Cancer Cell Growth. journal of biomedical science. 2011; 18(88)

25. Wloga D, Gaertig J. Post-translational modifications of microtubules. Journal of Cell Science. 2010; 123(20):3447–3455. [PubMed: 20930140]

26. Afjehi-Sadat L, Brejnikow M, Kang SU, Vishwanath V, Walder N, Herkner K, Redl H, Lubec G. Differential Protein Levels and Post-Translational Modifications in Spinal Cord Injury of the Rat. Journal of Proteome Research. 2010; 9(3):1591–1597. [PubMed: 20141154]

27. Sahab ZJ, Hall MD, Sung YM, Dakshanamurthy S, Ji Y, Kumar D, Byers SW. Tumor suppressor RARRES1 interacts with cytoplasmic carboxypeptidase AGBL2 to regulate the a-tubulin tyrosination cycle. Cancer Research. 2011; 71(4):1219–1228. [PubMed: 21303978]

28. Flavin M, Murofushi H. Tyrosine Incorporation in Tubulin. Methods in Enzymology. 1984; 106:223–237. [PubMed: 6387372]

29. Paturlelafanechere L, Manier M, Trigault N, Pirollet F, Mazarguil H, Job D. Accumulation of Delta-2-Tubulin, a Major Tubulin Variant That Cannot Be Tyrosinated, in Neuronal Tissues and in Stable Microtubule Assemblies. Journal of Cell Science. 1994; 107:1529–1543. [PubMed: 7962195]

30. Janke C, Rogowski K, Wloga D, Regnard C, Kajava AV, Strub JM, Temurak N, van Dijk J, Boucher D, van Dorsselaer A, Suryavanshi S, Gaertig J, Edde B. Tubulin polyglutamylase enzymes are members of the TTL domain protein family. Science. 2005; 308(5729):1758–1762. [PubMed: 15890843]

31. Redeker V, Rossier J, Frankfurter A. Posttranslational modifications of the C-terminus of alpha-tubulin in adult rat brain: alpha 4 is glutamylated at two residues. Biochemistry. 1998; 37(42): 14838–14844. [PubMed: 9778358]

32. Verdier-Pinard P, Wang F, Martello L, Burd B, Orr GA, Horwitz SB. Analysis of tubulin isotypes and mutations from taxol-resistant cells by combined isoelectrofocusing and mass spectrometry. Biochemistry. 2003; 42(18):5349–5357. [PubMed: 12731876]

33. Redeker V, Frankfurter A, Parker SK, Rossier J, Detrich HW. Posttranslational modification of brain tubulins from the antarctic fish Notothenia coriiceps: Reduced C-terminal glutamylation

correlates with efficient microtubule assembly at low temperatures. Biochemistry. 2004; 43(38): 12265–12274. [PubMed: 15379565]

34. Edde B, Rossier J, Lecaer JP, Desbruyeres E, Gros F, Denoulet P. Posttranslational Glutamylation of Alpha-Tubulin. Science. 1990; 247(4938):83–85. [PubMed: 1967194]
35. Redeker V, Lecaer JP, Rossier J, Prome JC. Structure of the Polyglutamyl Side-Chain Posttranslationally Added to Alpha-Tubulin. Journal of Biological Chemistry. 1991; 266(34): 23461–23466. [PubMed: 1720781]
36. Rudiger A, Rudiger M, Weber K, Schomburg D. Characterization of Posttranslational Modifications of Brain Tubulin by Matrix-Assisted Laser Desorption/Ionization Mass-Spectrometry - Direct One-Step Analysis of a Limited Subtilisin Digest. Analytical Biochemistry. 1995; 224(2):532–537. [PubMed: 7537474]
37. Rudiger AH, Rudiger M, Carl UD, Chakraborty T, Roepstorff P, Wehland J. Affinity mass spectrometry-based approaches for the analysis of protein-protein interaction and complex mixtures of peptide-ligands. Analytical Biochemistry. 1999; 275(2):162–170. [PubMed: 10552900]
38. Mao H, ElBissati K, Verdier-Pinard P, Burd B, Zhang HS, Kim K, Fiser A, Angeletti RH, Weiss LM. Post-Translational Modifications to Toxoplasma gondii alpha- and beta-Tubulins Include Novel C-Terminal Methylation. Journal of Proteome Research. 2010; 9(1):359–372. [PubMed: 19886702]
39. Sang Q-XA, Man Y-G, Sung YM, Khamis ZI, Zhang L, Lee M-H, Byers SW, Sahab ZJ. Non-receptor tyrosine kinase 2 reaches its lowest expression levels in human breast cancer during regional nodal metastasis. Clinical & experimental metastasis. 2012; 29(2):143–53. [PubMed: 22116632]
40. Sahab ZJ, Man YG, Semaan SM, Newcomer RG, Byers SW, Sang QXA. Alteration in protein expression in estrogen receptor alpha-negative human breast cancer tissues indicates a malignant and metastatic phenotype. Clinical and Experimental Metastasis. 2010; 27(7):493–503. [PubMed: 20602252]
41. Khamis ZI, Sahab ZJ, Byers SW, Sang QX. Novel Stromal Biomarkers in Human Breast Cancer Tissues Provide Evidence for the More Malignant Phenotype of Estrogen Receptor-Negative Tumors. Journal of Biomedicine and Biotechnology. 2011 Article ID 723650.
42. Sahab ZJ, Suh Y, Sang QXA. Isoelectric point-based prefractionation of proteins from crude biological samples prior to two-dimensional gel electrophoresis. Journal of Proteome Research. 2005; 4(6):2266–2272. [PubMed: 16335975]
43. Khamis ZI, Iczkowski KA, Sahab ZJ, Sang QXA. Protein profiling of isolated leukocytes, myofibroblasts, epithelial, Basal, and endothelial cells from normal, hyperplastic, cancerous, and inflammatory human prostate tissues. Journal of Cancer. 2010; 1:70–79. [PubMed: 20842227]
44. Sahab ZJ, Hall MD, Zhang L, Cheema A, Byers SW. Tumor Suppressor RARRES1 Regulates DLG2, PP2A, VCP, EB1, and Ankrd26. Journal of Cancer. 2010; 1(1):14–22. [PubMed: 20842219]
45. Zhu P, Bowden P, Zhang D, Marshall JG. MASS SPECTROMETRY OF PEPTIDES AND PROTEINS FROM HUMAN BLOOD. Mass Spectrometry Reviews. 2011; 30(5):685–732.
46. Mahn A, Ismail M. Depletion of highly abundant proteins in blood plasma by ammonium sulfate precipitation for 2D-PAGE analysis. Journal of Chromatography B-Analytical Technologies in the Biomedical and Life Sciences. 2011; 879(30):3645–3648.
47. Marco-Ramell A, Bassols A. Enrichment of low-abundance proteins from bovine and porcine serum samples for proteomic studies. Research in Veterinary Science. 2010; 89(3):340–343. [PubMed: 20371090]
48. Hu Y, Gopal A, Lin K, Peng Y, Tasciotti E, Zhang X, Ferrari M. Microfluidic enrichment of small proteins from complex biological mixture on nanoporous silica chip. Biomicrofluidics. 2011; 5(1)
49. Theilacker N, Roller EE, Barbee KD, Franzreb M, Huang X. Multiplexed protein analysis using encoded antibody-conjugated microbeads. Journal of the Royal Society Interface. 2011; 8(61): 1104–1113.

50. Choi S, Huang S, Li J, Chae J. Monitoring protein distributions based on patterns generated by protein adsorption behavior in a microfluidic channel. Lab on a Chip. 2011; 11(21):3681–3688. [PubMed: 21922107]
51. Choi S, Goryll M, Sin LYM, Wong PK, Chae J. Microfluidic-based biosensors toward point-of-care detection of nucleic acids and proteins. Microfluidics and Nanofluidics. 2011; 10(2):231–247.
52. Yang J-I, Huang H-Y, Chou Y-C, Chen C-C, Lee G-C, Chang H-W. Rapid and Economic DNA Extraction from a Single Salmon Egg for Real-Time PCR Amplification. Bioscience Biotechnology and Biochemistry. 2011; 75(10):2014–2017.
53. Dookeran NN, Yalcin T, Harrison AG. Fragmentation reactions of protonated alpha-amino acids. J of Mass Spectrom. 1996; 31(5):500–508.
54. Harrison AG. Ion chemistry of protonated glutamic acid derivatives. Int J of Mass Spectrom. 2001; 210(1-3):361–370.
55. Vinh J, Langridge JI, Bre MH, Levilliers N, Redeker V, Loyaux D, Rossier J. Structural characterization by tandem mass spectrometry of the posttranslational polyglycylation of tubulin. Biochemistry. 1999; 38(10):3133–3139. [PubMed: 10074368]
56. Calligaris D, Villard C, Terras L, Braguer D, Verdier-Pinard P, Lafitte D. MALDI In-Source Decay of High Mass Protein lsoforms: Application to alpha- and beta- Tubulin Variants. Analytical Chemistry. 2010; 82(14):6176–6184. [PubMed: 20552990]
57. Redeker V, Rusconi F, Mary J, Prome D, Rossier J. Structure of the C-terminal tail of alpha-tubulin: Increase of heterogeneity from newborn to adult. Journal of Neurochemistry. 1996; 67(5): 2104–2114. [PubMed: 8863520]
58. Jung SY, Li YH, Wang Y, Chen Y, Zhao YM, Qin J. Complications in the assignment of 14 and 28 Da mass shift detected by mass spectrometry as in vivo methylation from endogenous proteins. Analytical Chemistry. 2008; 80(5):1721–1729. [PubMed: 18247584]
59. Nogales E, Wolf SG, Downing KH. Structure of the alpha beta tubulin dimer by electron crystallography. Nature. 1998; 391(6663):199–203. [PubMed: 9428769]
60. Starling D. EFFECTS OF MITOTIC INHIBITORS ON STRUCTURE OF VINBLASTINE-INDUCED TUBULIN PARACRYSTALS FROM SEA-URCHIN EGGS. Journal of Cell Science. 1976; 20(1):91–100. [PubMed: 942955]
61. Chen JJ, Wang Z, Li CM, Lu Y, Vaddady PK, Meibohm B, Dalton JT, Miller DD, Li W. Discovery of Novel 2-Aryl-4-benzoyl-imidazoles Targeting the Colchicines Binding Site in Tubulin As Potential Anticancer Agents. Journal of Medicinal Chemistry. 2010; 53(20):7414–7427. [PubMed: 20919720]
62. Jourdan F, Leese MP, Dohle W, Hamel E, Ferrandis E, Newman SP, Purohit A, Reed MJ, Potter BVL. Synthesis, Antitubulin, and Antiproliferative SAR of Analogues of 2-Methoxyestradiol-3,17-O,O-bis-sulfamate. Journal of Medicinal Chemistry. 2010; 53(7):2942–2951. [PubMed: 20225862]

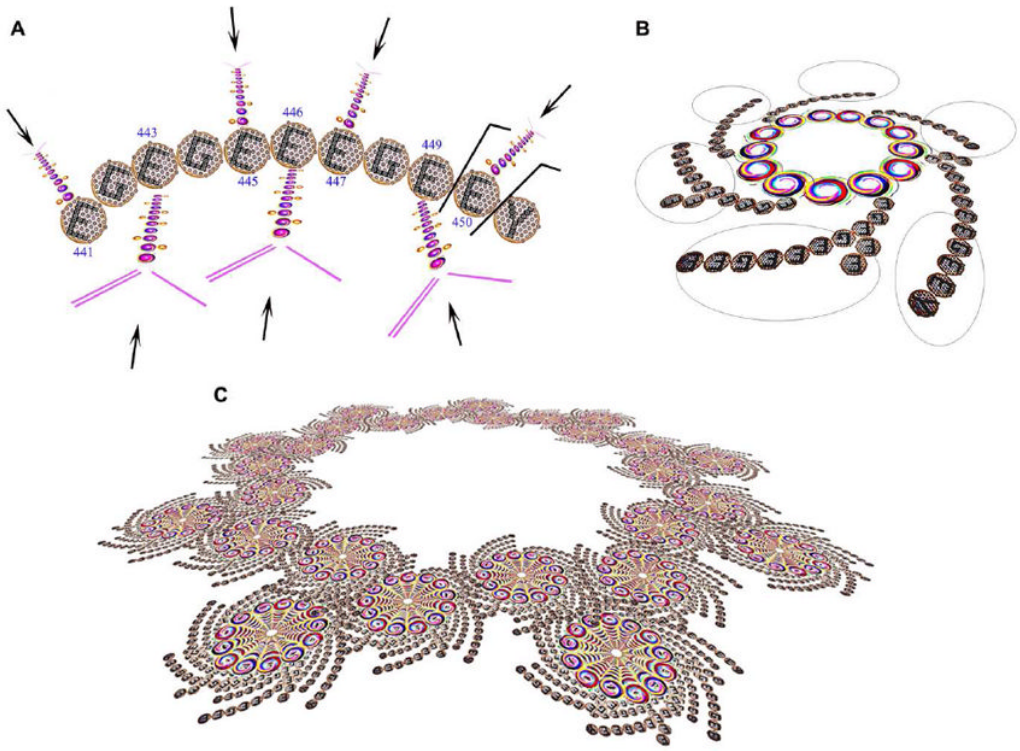

Figure 1.

C-Terminal Tail of mammalian tubulin-$\alpha_{1A/1B}$ structure and function. (A) Tubulin-$\alpha_{1A/1B}$ CTT has 7 glutamic acid residues that can potentially be modified by post-translational glutamate addition to their γ-carboxylic side chains (arrows). Other modifications includes the cleavage of C-terminal tyrosine (Y^{451}) resulting in the detyrosinated form of tubulin-$\alpha_{1A/1B}$ and the cleavage of E^{450} resulting in Δ2- tubulin-$\alpha_{1A/1B}$ (EGEGEEEGE). (B) Microtubules are composed of tubulin-α/β dimers. Their CTT (circled) is positioned at the outer lattice of microtubules suggesting that modification of this CTT regulates their interaction with microtubule-associated proteins (MAPS). (C) Centrioles are composed of nine microtubule triplets and play a major role during the mitotic progression, spindle assembly, proper positioning of the nucleus, and segregation of chromosomes. Modification of tubulin CTTs present at the outer lattice of centrioles will affect the interaction of centrioles with other biomolecules resulting in a regulation of their dynamics.

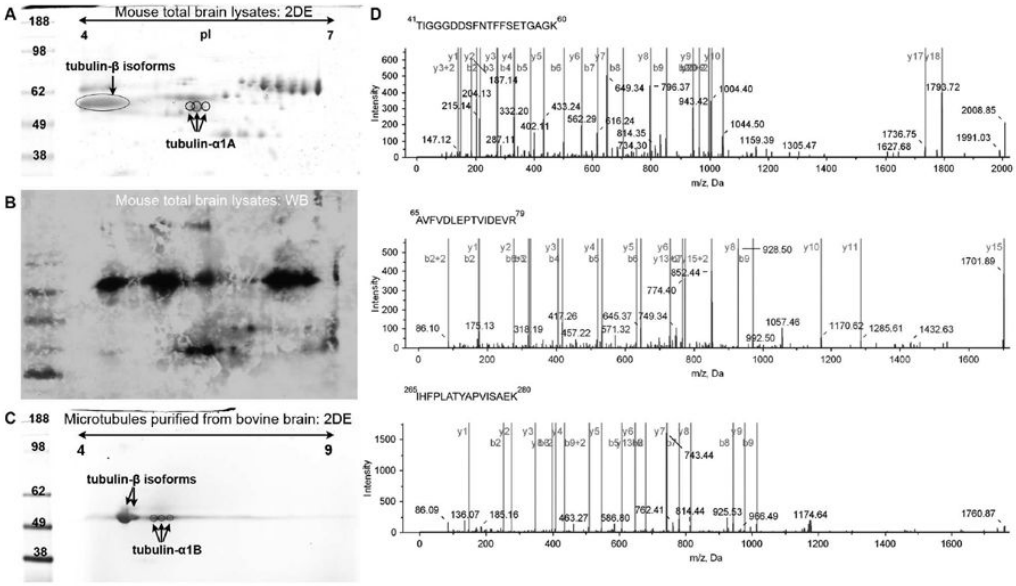

Figure 2.

Tubulin-$\alpha_{1A/1B}$ separation and identification. (A) Coomassie blue-stained 2-DE of proteins extracted from mouse brain tissues. Proteins were separated using a 7 cm Immobilized pH Gradient (IPG) strips, pH 4 to 7 in the first dimension and a 4-12% gradient polyacrylamide gel in the second dimension. Circled spots were identified as tubulin-$\alpha_{1A/1B}$ following trypsin digestion and ESI-TOF/TOF analysis. (B) 2-Dimensional western blot of mouse brain extracts against tubulin-α isoforms. (C) 2DE of a bovine microtubule sample (99% pure). (D) b- and y-type MS/MS fragmentation ions measured following ESI-TOF/TOF CID of 3 trypsin-generated tubulin peptides. The 3 ions were identified as residues 41 to 60; 65 to 79; and 265 to 280 of tubulin-$\alpha_{1A/1B}$ and as a result the 2DE spot was identified by Paragon as tubulin-$\alpha_{1A/1B}$.

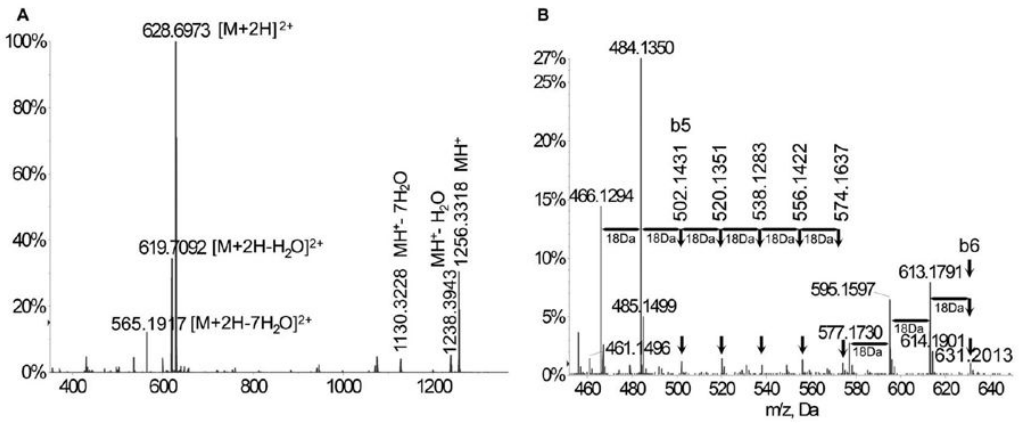

Figure 3.

Ionization, fragmentation pattern, and serial neutral loss in primary and CID MS/MS of synthetic tubulin-$\alpha_{1A/1B}$ CTT (EGEGEEEGEEY). (A) ESI-MS spectrum showing the singly charged synthetic CTT ion at m/z 1256.3318 and the double charged ion $[M+2H]^{2+}$ at m/z 628.6973. Neutral losses of 1 water molecule were observed in both single-charged $[M+H-H_2O]^{+}$ (m/z 1238.3943) and double-charged $[M+2H-H_2O]^{2+}$ (m/z 619.7092) ions. Neutral losses of up to 7 water molecules were also detected for both ions: $[M+2H-7H_2O]^{2+}$ (m/z 565.1917); $[M+H-7H_2O]^{+}$ (m/z 1130.3228). (B) A close-up look at the CID MS/MS spectra of EGEGEEEGEEY showed 3x18Da neutral losses for b6 (m/z 631.2013) and 2x18Da loss for b5 fragments (m/z 502.1431) and a pattern of 7 peaks from m/z 466.1294 to m/z 574.1637 with a ΔM of 18Da.

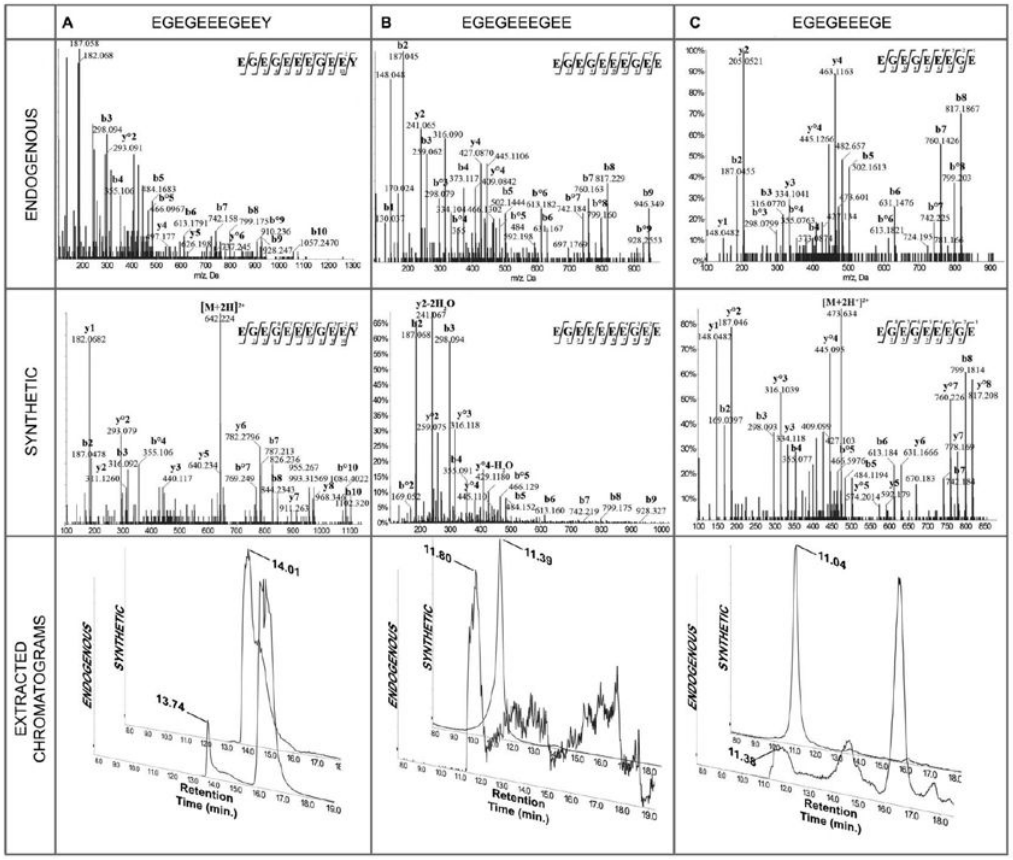

Figure 4.

CID MS/MS of endogenous (top), synthetic (middle), and extracted chromatograms (bottom) of (A) tyrosinated tubulin-$\alpha_{1A/1B}$ CTT: precursor ions were doubly charged at m/z 619.7040 for the synthetic peptide (t_R 14.01 min.) with a neutral loss of H_2O, and m/z 642.7346 for the endogenous one (t_R 13.74 min.) with 2 methylations; extracted ions created by targeting these 2 ions showed close retention times; (B)detyrosinated tubulin-$\alpha_{1A/1B}$ CTT: precursor ions were doubly charged at m/z 547.1812 for the synthetic peptide (t_R 11.39 min.) with 2 neutral losses of H_2O, and singly charged at m/z 1075.3301 for the endogenous one (t_R 11.80 min.) with 2 neutral losses of H_2O; extracted ions created by targeting these 2 ions showed close retention times; (C) Δ2-tubulin-$\alpha_{1A/1B}$ CTT: precursor ions were doubly charged at m/z 482.6544 for the synthetic peptide (t_R 11.04 min), and doubly charged at m/z 473.6524 for the endogenous one (t_R 11.38 min.) with 1 neutral loss of H_2O; extracted ions created by targeting these 2 ions showed close retention times. Fragmentation patterns of synthetic and endogenous peptides were similar after accounting for the methylation of endogenous peptides and the differential dehydration between endogenous and synthetic CTTs.

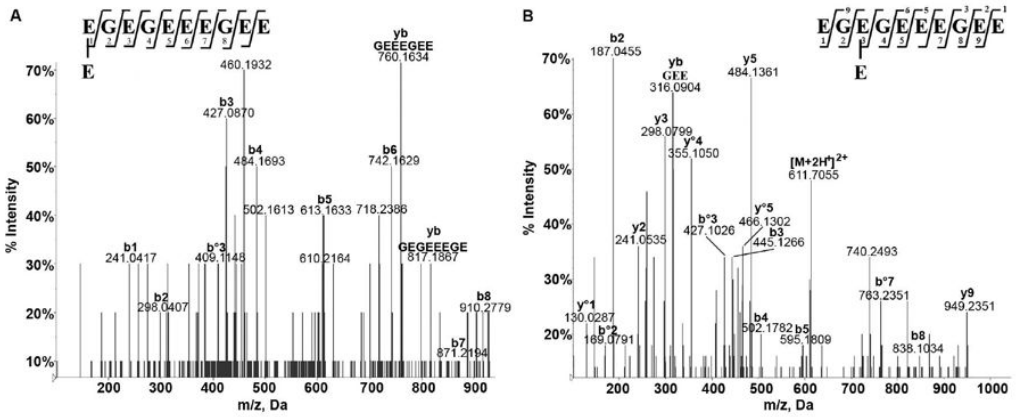

Figure 5.

Identification of novel glutamylation sites. CID MS/MS of detyrosinated tubulin-$\alpha_{1A/1B}$ CTT glutamylated at (A) E^{441} with a doubly charged precursor ion at m/z 609.7140, (B) E^{443} with a doubly charged precursor ion at m/z 611.6988. The difference in m/z is due to the differential methylation/dehydration between the two peptides.

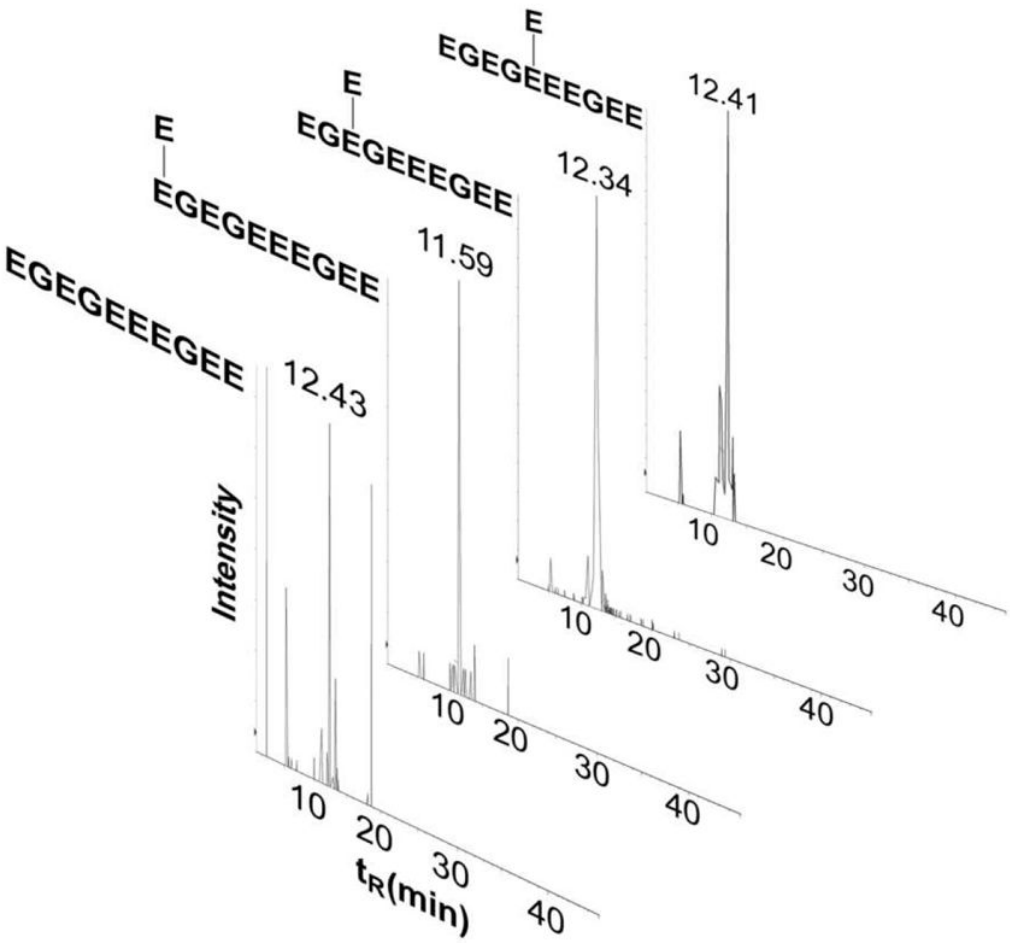

Figure 6.

Retention times of bovine detyrosinated/glutamylated tubulin-$\alpha_{1A/1B}$. Extracted ion chromatograms created by targeting detyrosinated and glutamylated tubulin-$\alpha_{1A/1B}$ CTTs including the newly identified CTT s glutamylated at E^{441} and E^{443} show close retention times in the range of 11.59-12.43 min that is close to the retention times of the endogenous (11.80 min.) and synthetic (11.39 min.) non-modified form of detyrosinated tubulin-$\alpha_{1A/1B}$ CTTs.

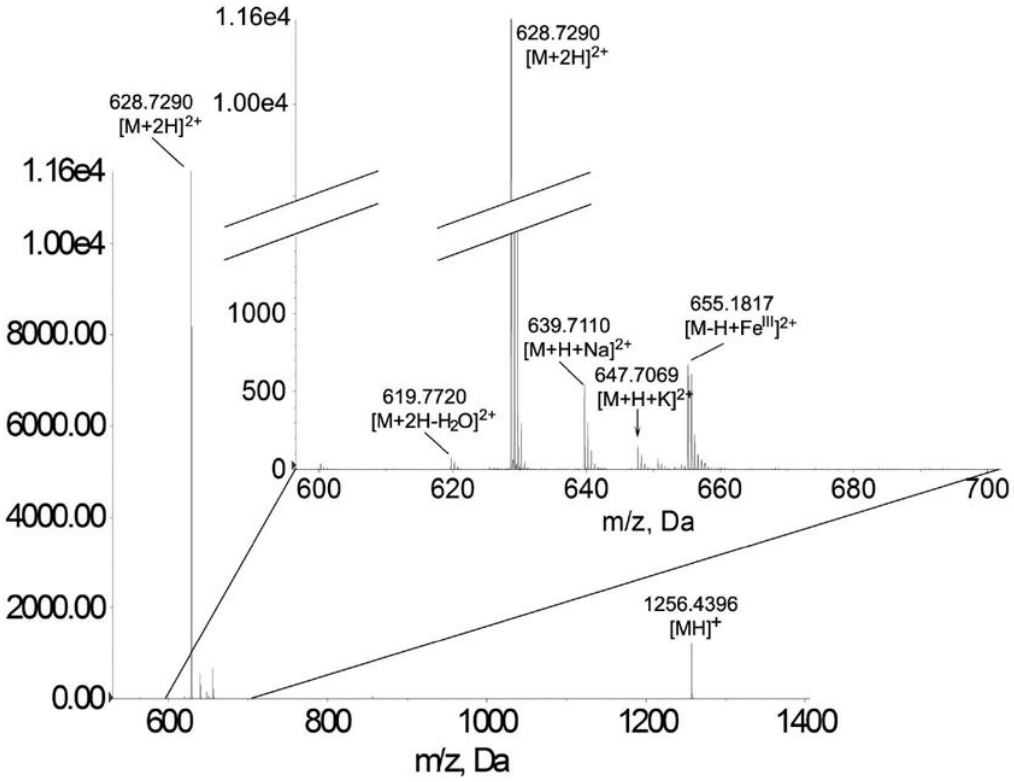

Figure 7.

Artifacts on tubulin-$\alpha_{1A/1B}$ glutamate CTT modifications. The following tyrosinated tubulin-$\alpha_{1A/1B}$ forms were detected: singly charged (m/z 1256.4396); double charged (m/z 628.7290); dehydrated/or pyroglutamylated ([M+2H-HO] m/z 619.7720); sodium adduct (m/z 639.7110); potassium adduct (m/z 647.7069); and iron adduct (m/z 655.1817).

Table 1

Identified mouse tubulin-$\alpha_{1A/1B}$ C-terminal structures and modifications

CTT Sequence	m/z obs	Mr Calc.	Error (Da)	z	Score	Expect	Figure	Artifact	Neutral loss	Methylation
EGEGEEEGEEY	647.8165	1293.5010	0.1174	2	14	0.017	S4	E441 (-H2O)	2 × 18 Da	E443/5/6/9
EGEGEEEGEE	561.2867	1120.4169	0.1565	2	15	0.049	S5	-	2 × 18 Da	E446/C-term
EGEGEEEGE	326.8238	977.3713	0.1003	3	20	0.0067	S6	-	4 × 18 Da	C-term
E | EGEGEEEGEE	406.8214	1217.4333	0.0308	3	27	0.005	S7	E on E441 (-H2O)	2 × 18 Da	E447
E | EGEGEEEGEE	426.8490	1277.4908	0.0562	3	20	0.032	S8	-	2 × 18 Da	E441/5/50/C-term
E | EGEG(EEE)GEE	417.4574	1249.4973	0.1250	3	24	0.013	S9	-	4 × 18 Da	E446/C-term
2E | EGEGEEEGEE	465.1938	1392.5555	0.0258	3	33	0.0032	S10	-	4 × 18 Da	E445
E | EGEGEEEGEEY	461.1760	1380.5092	0.0188	3	34	0.00038	S11	E on E441 (-H2O)	4 × 18 Da	E445
E | EGEG(EEE)GEEY	490.5146	1468.5729	0.0292	3	32	0.00026	S12	-	-	E446/7/9/50/C-term/E on E445
E | EGEGEEEGEEY	495.2370	1482.6011	0.1100	3	23	0.0032	S13	-	2 × 18 Da	E441/6/7/9/50/C-term/E on E443
EGEGEEEGEEY	642.7346	1283.4677	0.0015	2	57	0.0000041	Fig. 4A	-	-	E446/7
EGEGEEEGEE	1075.3301	1074.3751	0.045	1	66	0.0000018	Fig. 4B	E441 (-H2O)	2 × 18 Da	-
EGEGEEEGE	473.6524	945.3199	0.0151	2	60	0.0000091	Fig. 4C	E441 (-H2O)	-	-

Table 2

Identified bovine tubulin-$\alpha_{1A/1B}$ C-terminal structures and modifications

CTT Sequence	m/z obs	Mr Calc.	Error (Da)	z	Score	Expect	Figure	Artifact	Neutral loss	Methylation
EGEGEEEGEEY	447.5745	1339.5303	0.1932	3	26	0 00063	S14	-	-	E441/3/7/9/50 C-term
EGEGEEEGEE	383.7725	1148.4608	0.1433	3	20	0.011	S15	-	4 × H2O	E441/3/7 C-term
EGEGEEEGE	326.7499	977.3713	0.1216	3	34	0.00028	S16	-	2 × H2O	E447
E | EGEGEEEGEE	416.2027	1245.4772	0.1309	3	26	0.008	S17	E on E441 (-H2O)	4 × H2O	E446/50 C-term
E | EGEGEEEGEE	402.2155	1203.4554	0.1911	3	16	0.025	S18	E441 (-H2O)	6 × H2O	-
E | EGEG(EEE)GEE	623.7271	1245.4646	0.0104	2	22	0.029	S19	E441 (-H2O)	2 × H2O	E447/9 E on E445
E | EGEGEEEGEEY	476.5011	1426.5385	0.0352	3	42	6.6e-005	S20	-	2 × H2O	E443/5 E on E441
E | EGEGEEEGEE	609.714	1217.4207	0.0073	2	23	0.042	Fig. 5A	E on E441 (-H2O)	-	C-term
E | EGEGEEEGEE	611.6988	1221.466	0.0684	2	25	0.0025	Fig. 5B	-	6 × H2O	-